



Low- $\delta^{18}\text{O}$ Neoproterozoic precipitation recorded in a 2.67 Ga magmatic-hydrothermal system of the Keivy granitic complex, Russia

D.O. Zakharov^{a,*}, D.R. Zozulya^b, D. Rubatto^{a,c}

^a Institute of Earth Sciences, University of Lausanne, Lausanne, CH-1015, Switzerland

^b Geological Institute, Kola Science Centre of the Russian Academy of Sciences, Apatity, 184209, Russia

^c Institute of Geological Sciences, University of Bern, Baltzerstrasse 3, Bern, CH-3012, Switzerland



ARTICLE INFO

Article history:

Received 6 July 2021

Received in revised form 16 November 2021

Accepted 25 November 2021

Available online 15 December 2021

Editor: B. Wing

Keywords:

oxygen isotopes

Archean

peralkaline granites

low $\delta^{18}\text{O}$ systems

ABSTRACT

The modern hydrological cycle includes precipitation of ^{18}O -depleted meteoric water over continental crust exposed above sea-level. How far back in the geological record can continental exposure be documented remains uncertain, particularly for the Archean. To investigate the extent of Archean continental exposure, we document a newly discovered low- $\delta^{18}\text{O}$ magmatic-hydrothermal system that was emplaced in a shallow crust of the Keivy complex, Kola craton at 2.67 Ga. This study builds a case for syn-emplacement hydrothermal exchange with the local meteoric water that had $\delta^{18}\text{O}$ at least as low as -11‰ VSMOW. Coupled with the high-latitude position of the Kola craton at the time, this result presents a paleogeographic documentation of continental exposure and a quantitative estimate of the isotope composition of Neoproterozoic precipitation. We employ detailed $\delta^{18}\text{O}$ mapping using mineral separates and bulk samples, as well as ion microprobe $\delta^{18}\text{O}$ measurements and U-Pb dating of zircon. The spatially extensive O-isotope dataset ($n = 63$) spans over 120 km in length across different lithological units including the peralkaline granites of the Keivy complex, the hosting gneiss and contact hydrothermal quartzolites. All analyzed samples, including whole rock samples and mineral separates, show $\delta^{18}\text{O}$ below those expected for mantle- and crust-derived magmas. The lowest $\delta^{18}\text{O}$ of ca. -7‰ are measured in minerals and bulk rock of the altered gneisses near the intrusive contacts. Peralkaline granites returned $\delta^{18}\text{O}$ values ranging between -6 and $+5\text{‰}$. Zircon crystals with preserved igneous zoning have low $\delta^{18}\text{O} = +2.2\text{‰}$ and yield an emplacement age for the magmatic complex of 2672 ± 7 Ma. Zircon dating from quartzolites at the contact between granites and country gneisses points to fluid-rock interaction at 2.67 and at 1.77–1.79 Ga. We propose that the spatially extensive O-isotope depletion documents a Neoproterozoic shallow magmatic-hydrothermal system where magmatic assimilation produced the low- $\delta^{18}\text{O}$ granites and the hydrothermal cycling of meteoric water in the ambient crust resulted in formation of low- $\delta^{18}\text{O}$ altered host rocks. Since the lowest $\delta^{18}\text{O}$ value measured in a rock is ca. -7‰ , the equilibrium fluids had $\delta^{18}\text{O}$ of around -9‰ under hydrothermal conditions (300–400 °C) characteristic for the shallow crust around cooling intrusions. Considering that hydrothermal fluids are shifted 1–2‰ towards higher values, the contemporaneous precipitation had $\delta^{18}\text{O} = -11\text{‰}$ or lower. Consequently, the 2.67 Ga Keivy complex is the earliest known intact low- $\delta^{18}\text{O}$ magmatic-hydrothermal system offering a quantitative record of the Neoproterozoic precipitation that can be used as a tool in paleogeographic reconstructions.

© 2021 The Author(s). Published by Elsevier B.V. This is an open access article under the CC BY license (<http://creativecommons.org/licenses/by/4.0/>).

1. Introduction

Active and subaerially exposed shallow magmatic-hydrothermal systems document an intimate interaction between magma reservoirs and low- $\delta^{18}\text{O}$ surface waters. The investigations of these sys-

tems show that storage of magmas in shallow continental crust promotes heating that in turn launches hydrothermal cycling of groundwater, re-melting and assimilation of the near-surface altered lithologies (Bindeman et al., 2008; Troch et al., 2020). Particularly demonstrative interactions are subaerial caldera-forming eruptions, and subsequent remelting of the low- $\delta^{18}\text{O}$ inter-caldera fill that was altered in contact with surface water (Bindeman et al., 2008; Watts et al., 2012). The striking feature of surface altered materials is due to the O isotope signature of meteoric water that

* Corresponding author.

E-mail address: david.zakharov@unil.ch (D.O. Zakharov).

has markedly low $\delta^{18}\text{O}$, mostly between -60 and -2‰ , with the lower values found progressively closer towards higher latitudes (Craig, 1961; Dansgaard, 1964; Rozanski et al., 1993). Such negative values are distinct from that of seawater ($\delta^{18}\text{O} \approx 0\text{‰}$) and of unaltered magmatic rock ($\delta^{18}\text{O} = +6$ to $+11\text{‰}$, Taylor, 1977). During hydrothermal alteration at temperatures between 300 and 600 °C , the low- $\delta^{18}\text{O}$ signature of local precipitation is incorporated into secondary minerals via high-temperature exchange reactions. Upon further heating, re-melting and assimilation of such hydrothermally altered rocks, this low- $\delta^{18}\text{O}$ signature is transferred to the newly generated melts. For example, modern altered crust in the Krafla system in Iceland bears low $\delta^{18}\text{O}$ values between -11 and -5‰ due to exchange with the local precipitation ($\delta^{18}\text{O} = -12\text{‰}$), while the erupted rhyolites have $\delta^{18}\text{O}$ range of $+1$ to $+3\text{‰}$ (Zakharov et al., 2019 and references therein). In another example, the magmas produced at the Yellowstone track hotspot calderas reach down to values of around -1‰ , clearly marking a strong signature of incorporating low- $\delta^{18}\text{O}$ hydrothermally altered rocks (Watts et al., 2012). Due to the high-temperature exchange between surface water and crustal rocks, the O isotope systematics of ancient hydrothermal-magmatic systems can assist in the reconstruction of ancient hydrological patterns, especially when no other proxy is available for the climate conditions. The Archean climate is specifically controversial due to the scarcity and preservation issues of the traditional sedimentary proxies, i.e. marine carbonates.

Large long-lived magmatic-hydrothermal systems likely existed through the geologic history, while substantial continental exposure and, thus, low- $\delta^{18}\text{O}$ precipitation over continental land emerged sometime in the Precambrian history. This likely occurred during late Archean to early Proterozoic when lithospheric strength matured promoting continental hypsometry (Flament et al., 2008; Bindeman et al., 2018; Spencer et al., 2019). The exact timing and extent of emergence of continental crust is currently poorly constrained, yet it is critical for understanding of how the habitable environments changed on Earth, and linking geodynamics, magma production, surface processes and long-term climate evolution (Dhuime et al., 2012; Johnson and Wing, 2020; Catling and Zahnle, 2020). Due to poor preservation of ancient continental blocks and scarcity of methods that can directly reconstruct the areal exposure, it is especially difficult to estimate the extent of the Archean continental crust.

To address this uncertainty, we investigate a Neoproterozoic magmatic-hydrothermal system and document its emplacement in sub-aerially-exposed crust, presenting constraints on the $\delta^{18}\text{O}$ of ancient meteoric water. In modern-day world, the governing factor that controls $\delta^{18}\text{O}$ value of meteoric water is temperature (Craig, 1961; Dansgaard, 1964). Another important factor is 'continentality', i.e. the proximity of precipitation to ocean shore line, which is characterized by lower mean annual temperatures and lower $\delta^{18}\text{O}$ values of precipitation measured inland compared to the coastal areas (Rozanski et al., 1993; Winnick et al., 2014). Today the largest continent Asia with its diverse topography and $\sim 45 \cdot 10^6 \text{ km}^2$ area is characterized by $\delta^{18}\text{O}$ gradients of precipitation between 0 and -30‰ , with the lowest values found deep inland (Rozanski et al., 1993). Thus, by finding low- $\delta^{18}\text{O}$ magmatic-hydrothermal complexes in the Archean, during or before the proposed temporal intervals of continental emergence, we can gain at least a comparative constraint on the surface temperatures and the extent of subaerial continental exposure. Previous work showed that some continental crust was exposed based on detrital grains of zircons with low $\delta^{18}\text{O}$ values (e.g. Hammerli et al., 2018; Wang et al., 2021), hinting at the presence of subaerial high-temperature hydrosphere-rock interaction dating back to the Meso- and Neoproterozoic. These studies provide evidence for meteoric water-rock interactions, but due to the detrital nature of the low $\delta^{18}\text{O}$ zircon grains, it is difficult to place quantitative con-

straints on hydrosphere isotope values in situ (i.e. $\delta^{18}\text{O}$ of meteoric water). While detrital zircons represent an important archive of long-term evolution of hydrosphere-crust interaction (Spencer et al., 2019; Wang et al., 2021), the uncertain provenance of detrital low- $\delta^{18}\text{O}$ zircons makes it difficult to assess the mechanisms of incorporating meteoric water signals, either via recycling of pre-existing or syn-magmatic low $\delta^{18}\text{O}$ rocks, thus, the timing and the extent of subaerial water-rock reactions are not always evident. The investigated here shallow hydrothermal-magmatic system of Archean age has a potential to clarify the climate and hydrological conditions that are otherwise hard to probe with traditional proxies.

In this paper, we provide large-scale oxygen isotope documentation of a shallow magmatic-hydrothermal system that was generated in an orogenic setting at 2.67 Ga on the Kola craton of the Baltic (Fennoscandian) Shield (Fig. 1). The magmatic activity produced large granitic bodies of peralkaline composition that now outcrop over the areal extent of 2500 km^2 forming the Keivy peralkaline granite province (Batieva, 1976; Zozulya et al., 2005). We show that the several granitic bodies collectively termed "Keivy granites" and their host rocks span in $\delta^{18}\text{O}$ between -7 to $+5\text{‰}$ and represent some of the lowest values measured in Archean formations. We provide detailed spatial $\delta^{18}\text{O}$ sampling across multiple lithological units, including the massive granites, and the contact areoles. Hydrothermal processes are manifested via late-stage hydrothermal veins and aggregates developed in near-contact areoles of the Keivy complex (Bagiński et al., 2016; Macdonald et al., 2017). We target the late-stage quartz-rich contact rocks (quartzolites hereinafter) that likely formed from late-stage hydrothermal fluids. We combine in situ zircon U-Pb dating of these lithologies, $\delta^{18}\text{O}$ mapping using mineral separates and whole rocks collected across the distance of $\sim 100 \text{ km}$ to determine the timing and conditions of the igneous emplacement and alteration. In addition, well-preserved igneous zircons were analyzed in situ for $\delta^{18}\text{O}$ to test for igneous recycling of the low- $\delta^{18}\text{O}$ materials.

2. Geological setting

The Keivy peralkaline granites crop out in the Keivy terrane, a fault-isolated fragment of crust on the Kola craton (NE Baltic Shield, Russia). The terrane is surrounded by the cratonic TTG (tonalite-trondhjemite-granodiorite) rocks in the north and by the Paleoproterozoic ($< 2.5 \text{ Ga}$) Imandra-Varzuga belt in the south (Fig. 1). The Keivy terrane includes voluminous peralkaline granites and mafic (gabbro-anorthosite) intrusions that intruded at ca. 2.67 Ga (Bayanova, 2004; Zozulya et al., 2005; Vetrin and Rodionov, 2009) and cut the suites of metavolcanic and metasedimentary sequences. In summary, the Keivy terrane records: (1) sedimentation and volcanism between ~ 2.9 - 2.7 Ga , (2) within-plate bimodal plutonic magmatism at 2.67 Ga , and (3) regional metamorphism at ca. 1.8 Ga , with minor episodes of recrystallization at $\sim 1.7 \text{ Ga}$ (Bayanova, 2004; Zozulya et al., 2005; Balagansky et al., 2021). The youngest 1.6 - 1.7 Ga event is traced by U-Th-Pb ages of monazite, xenotime, and zircon from hydrothermal veins and pegmatites, and is related to fluid-thermal activation of the Baltic Shield during this time (Bayanova, 2004; Macdonald et al., 2017).

The peralkaline granites and minor syenites represent one of the most voluminous formations of the Keivy terrane (Batieva, 1976). Within the terrane, the granitic bodies are subdivided into individual localities (Fig. 1): West Keivy, White Tundra, Lavrentievskii and Ponoiskii. They are composed of two-feldspar granites with alkaline mafic minerals, sometimes with K-Na-feldspar phenocrysts. The mafic minerals are arfvedsonite, aegirine, and biotite. Texturally, these rocks range from porphyritic to lineated, representing the distinction between well-preserved and recrystallized varieties (Fig. 2). It is assumed that recrystallization and

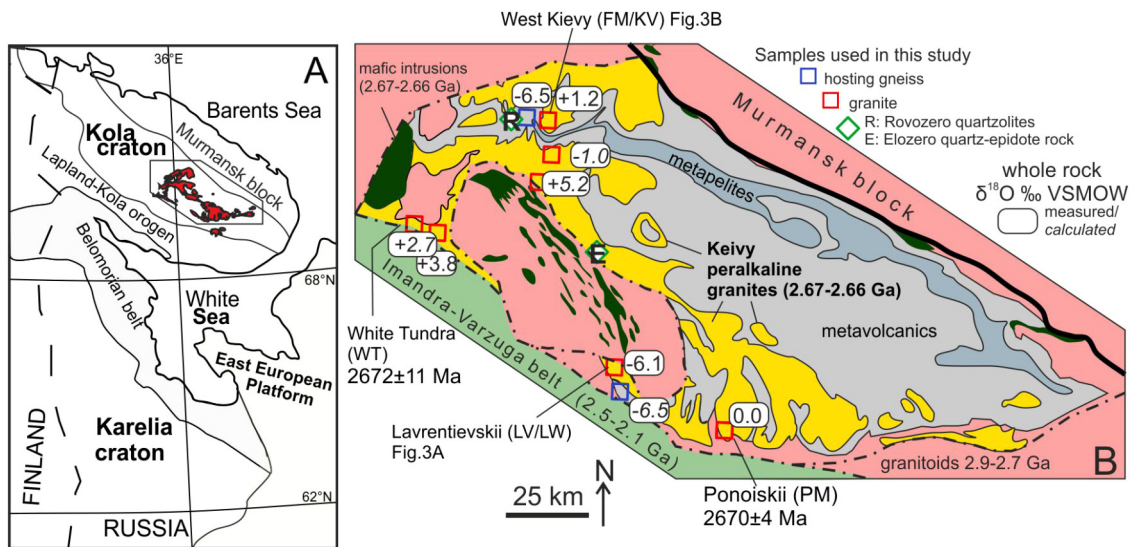


Fig. 1. **A** – Position of the 2.67 Keivy peralkaline granites (shown in red) in the structure of Fennoscandian Shield; **B** – Schematic map of the Keivy terrane. The 2.67 Ga peralkaline granites are shown in yellow along with the sampled localities. The lowest $\delta^{18}\text{O}$ values at each locality are shown as measured whole rock samples or calculated from quartz oxygen isotope measurements (*italics*). The ages of peralkaline granites determined here by U-Pb zircon geochronology are shown. Other units and their ages composing the Keivy terrane are shown. The ages of peralkaline granites and mafic intrusions are shown as 2.66–2.67 Ga and are based on previous investigations (Bayanova, 2004; Zozulya et al., 2005; Vetrin and Rodionov, 2009). The dashed-dotted lines signify faults. The thick black curve represents the structural boundary between the Keivy terrane and the Murmansk block. (For interpretation of the colors in the figure(s), the reader is referred to the web version of this article.)

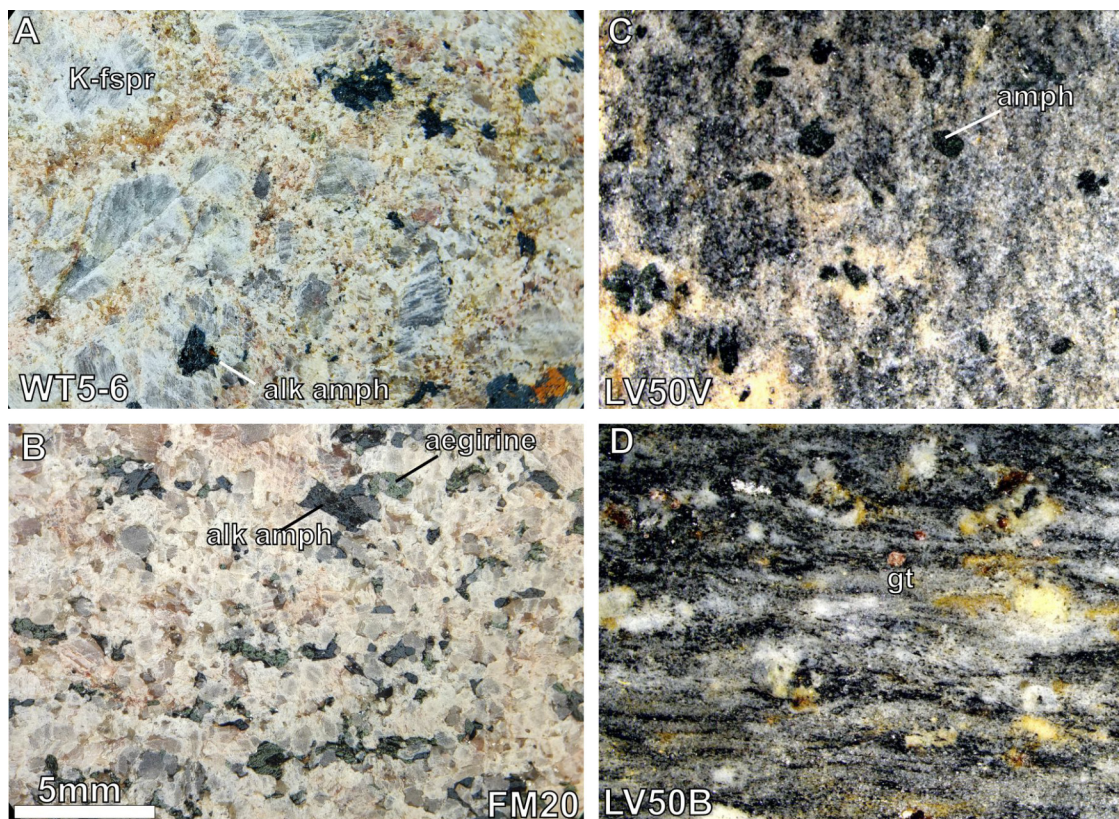


Fig. 2. Petrographic appearance of the sampled lithologies. The scale bar (5 mm; lower left corner) is applicable to all images. **A** – peralkaline granite with remaining K-Na-feldspar porphyritic texture from the White Tundra locality (sample WT5–6; $\delta^{18}\text{O}_{\text{amphibole}} = -1.3\text{‰}$ and $\delta^{18}\text{O}_{\text{quartz}} = 4.3\text{‰}$). Porphyry K-Na-feldspar (K-fsپر) and alkaline amphibole (alk amph) grains are shown. **B** – a recrystallized variety of peralkaline granite sampled at the West Keivy locality (sample FM20; $\delta^{18}\text{O}_{\text{quartz}} = -0.4$, $\delta^{18}\text{O}_{\text{aegirine}} = -4.5\text{‰}$, $\delta^{18}\text{O}_{\text{albite}} = -2.1\text{‰}$). **C** – a near-contact altered hosting gneiss that exhibits typical hastingsite porphyroblasts (sample LV50V; $\delta^{18}\text{O}_{\text{garnet}} = -7.3\text{‰}$ and $\delta^{18}\text{O}_{\text{amphibole}} = -7.8\text{‰}$). **D** – a typical sample of the hosting garnet-two-mica gneiss that does not exhibit petrographic features of alteration (sample LV50B; $\delta^{18}\text{O}_{\text{garnet}} = -1.9\text{‰}$ and $\delta^{18}\text{O}_{\text{muscovite}} = 1.6\text{‰}$).

lineation occurred at ca. 1.8 Ga when the Keivy terrane was subjected to amphibolite-facies metamorphism (Batieva, 1976). The host rocks of the Keivy granites are represented by metavolcanic garnet-biotite gneisses (Lebyazhka suite) derived from metamor-

phosed tuffs and lavas of rhyolitic and dacitic composition (Balagansky et al., 2021). The gneisses are altered in the vicinity of the intrusive contacts. The alteration is recognized by the presence of blueish hastingsite-type amphibole in the gneisses surrounding

the peralkaline granite intrusions (Fig. 2). The precise age of these gneisses is difficult to establish due to the lack of abundant zircon appropriate for dating. Previous efforts produced the age of 2871 ± 15 Ma for the hosting gneisses (Bayanova, 2004), suggesting that they significantly predate the intrusive Keivy granites. However, a more recent study by Balagansky et al. (2021) determined U-Pb zircon ages of 2678 ± 7 Ma from the hosting metatrachyrhyolites, and interpreted them as extrusion ages. This interpretation implies that the gneiss protolith would be near-contemporaneous to the peralkaline granites. Despite the disagreement of these dates and potential complications caused by zircon recrystallization in the altered gneisses, peralkaline granites intrusively cut the host rocks and thus, postdate them.

The peralkaline granites are spatially associated with quartzolites that tend to occur close to the contacts with the hosting rocks. Quartzolites form irregularly shaped bodies ranging in size from 1 to 10 s of meters across, emplaced both in granites and host rocks. The quartzolites represent quartz-rich (>50 vol.% quartz) aggregates with subordinate amounts of zircon, fergusonite, britholite, monazite and chevkinite. In some areas, they are spatially associated with pegmatites, but have no zonal structure. It is assumed that quartzolites form under conditions between pegmatitic to hydrothermal (Zozulya et al., 2020). In general, late-stage hydrothermal activity is widely distributed in form of quartz veins, pegmatites (both in granite bodies and in host rocks), metasomatic aureoles around granite bodies. These rocks are interpreted either as syngenetic with emplacement of peralkaline granites or postdating them at ~ 1.7 Ga (Macdonald et al., 2017). Due to enrichment in water and fluorine, the residual fluids of crystallized peralkaline granitic magma promoted formation of quartzolites with notable Zr-, Nb-, REE-, Y-, Th- and U-mineralization accompanied by extensive recrystallization and alteration of the contact granites and the hosting gneisses (Macdonald et al., 2017). Emanating fluids also affected the 2.67 Ga mafic intrusions, forming the quartz-epidote metasomatic rocks with abundant zircon and rare-metal minerals (Bagiński et al., 2016). The late-stage quartz-dominant rocks that were investigated include zircon-rich quartzolites from Rovozero and a quartz-epidote rock of the Elozero localities (see Fig. 1). The Rovozero locality contains quartzolites emplaced in the hosting gneisses, while the Elozero quartz-epidote rock formed at the contact between the peralkaline granite and an intrusion of gabbro-anorthosite (Zozulya et al., 2020).

3. Methods

3.1. Sample collection

The suite of samples collected in the field for this study includes peralkaline granites, associated quartzolites and host gneisses. In total 22 samples were used to extract individual mineral grains from lightly crushed rocks. Zircon crystals were separated from peralkaline granites, quartzolites, and a quartz-epidote contact metasomatic rock using crushing, magnetic and heavy liquid separation. In addition, 13 samples of peralkaline granites and host rocks were crushed and powdered for bulk rock analyses.

3.2. Laser fluorination $\delta^{18}\text{O}$ values

The $\delta^{18}\text{O}$ values of bulk rocks and mineral separates were determined by laser-assisted fluorination in the vacuum line and subsequent measurement at a mass spectrometer at the Institute of Earth Sciences, University of Lausanne. Samples (0.5–2 mg) were loaded in a Pt-tray holder either as whole rock powders or separated minerals. After heating in an oven to 110°C , the loaded Pt-tray was transferred into the sample chamber, where the air was evacuated. After resting under vacuum ($P \approx 10^{-6}$ mbar) for several

hours, the samples were pre-fluorinated in presence of ~ 50 mbar F_2 gas overnight to get rid of excess moisture. Extraction of O_2 gas was mediated via heating with CO_2 laser in presence of F_2 gas ($P \approx 100$ mbar). The extracted O_2 gas was transferred through a series of cryogenic traps and collected on a molecular sieve with 5 Å pore diameter. The collected oxygen was introduced into a MAT 253 mass spectrometer, where every measurement consisted of 8 cycles of comparisons between the reference and analyte O_2 gases. For monitoring the accuracy of measurements and for day-to-day corrections, the quartz standard LS1 ($\delta^{18}\text{O} = 18.1\text{‰}$ VSMOW; Jourdan et al., 2009) was routinely measured within every session. Typical reproducibility of LS1 standard was $<0.2\text{‰}$.

3.3. $\delta^{18}\text{O}$ zircon measurement by secondary ion mass spectrometry (SIMS)

The $\delta^{18}\text{O}$ values of zircons extracted from the peralkaline granite sample PM8 were determined in situ using the Cameca IMS 1270 secondary ion mass spectrometer equipped with cesium ion source installed at the CRPG-CNRS in Nancy, France. The zircon crystals were mounted in indium together with zircon standard 91500 ($\delta^{18}\text{O} = 9.9 \pm 0.1\text{‰}$; Wiedenbeck et al., 2004). Prior to mounting they were polished to expose the grain centers. The crystals were studied under a Scanning Electron Microscope (SEM) CamScan MV2300 to acquire back-scattered electron (BSE) and cathodoluminescent (CL) images. The targeted zircon crystals ($n = 7$) were selected based on the preservation of distinct igneous zoning in CL images. The analyses employed a 10 kV Cs^+ primary ion beam with a ~ 2 nA current focused on a ~ 8 μm diameter spot. Pre-sputtering of targeted areas during 45 s was applied with a 10 μm raster before each measurement. The secondary ions were extracted using negative 10 kV potential applied to the sample holder. The $^{18}\text{O}/^{16}\text{O}$ ratios were measured using the mass resolving power of ~ 2400 in a multi-collection mode using two off-axis L'2 and H1 Faraday cup (FC) detectors. The obtained ion intensities of ^{16}O and ^{18}O were 1.3×10^9 and 2.7×10^6 counts per second (cps) respectively. Additionally, we monitored the presence of water-containing domains in our Archean zircons using the $^{16}\text{OH}/^{16}\text{O}$ ratio. The $^{16}\text{OH}^-$ was detected on the axial electron multiplier (EM) detector using the MRP of 5000 to separate the interference from ^{17}O . Each measurement consisted of 30 cycles with counting time of 5 s per cycle. Four measurements of the 91500 standard were made in the beginning and the end of the session to monitor stability and accuracy of the analyses. Blocks of 4–5 unknowns were bracketed by 2–3 measurements of the 91500 zircon standard.

3.4. U-Pb zircon dating by SIMS

The U-Pb dating of zircon was conducted using the Cameca IMS 1280HR secondary ion probe mass spectrometer (SIMS) equipped with a high-brightness Hyperion H201 RF plasma oxygen ion source at the SwissSIMS facility of the University of Lausanne. Several tens of zircons extracted from each sample of the peralkaline granite and quartzolite were placed in the same amount that was used to investigate the sample PM8 for oxygen isotopes by SIMS. The mount included zircon standards 91500 and FC1.

The U-Pb ages were measured using a 5–7 nA O^{2-} -primary beam focused to a 20 μm spot. Secondary ions of ZrO, U, Th and Pb were extracted at 10 kV and measuring in mono-collection mode using the axial EM at a MRP of ~ 5000 . The reference zircon 91500 (1065 Ma; Wiedenbeck et al., 2004) was used as a standard for calibration using the $\text{UO}_2^+/ \text{U}^+$ vs Pb^+/ U^+ relative sensitivity calibration; the propagated calibration uncertainty was 1.26%. The secondary standard FC1 (1099.0 ± 0.6 Ma; Paces and Miller, 1993) was used to monitor the accuracy and returned a Concordia age of

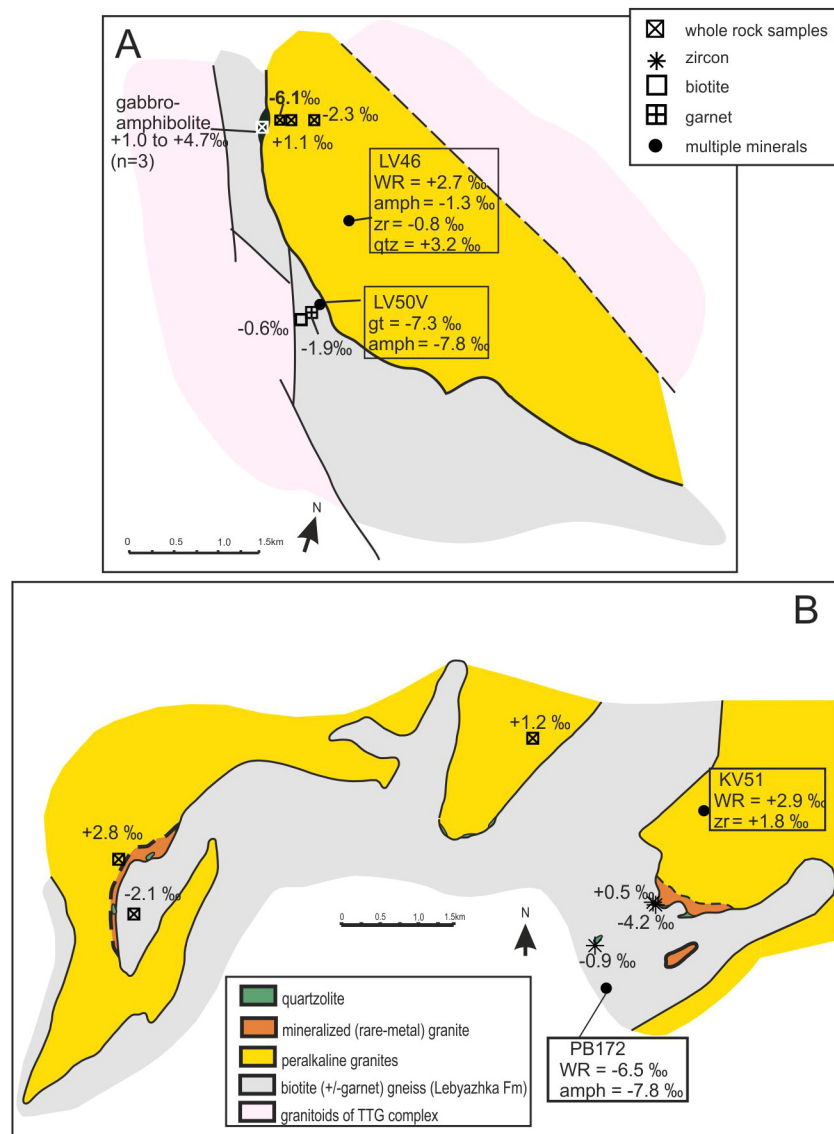


Fig. 3. The schematic illustrations of our $\delta^{18}\text{O}$ sampling at the near-contact areas. **A** – Lavrentievskii locality with $\delta^{18}\text{O}$ values determined in sampled peralkaline granites and their host rocks. **B** – West Keivy locality with $\delta^{18}\text{O}$ values measured in peralkaline granites, host rocks, and quartzolites. The abbreviations within the insets: WR = whole rock, amph = amphibole, gt = garnet, qtz = quartz, zr = zircon.

1101.7 \pm 5.2 Ma. Common Pb correction was based on the ^{204}Pb signals using the present-day terrestrial Pb composition (Stacey and Kramers, 1975). Data reduction was carried out using the CAMECA-CIPS software compiled by Martin Whitehouse at Nord-sim facility, and the results were plotted with IsoPlot Ex 4.15 (Ludwig, 2003).

4. Results

4.1. Bulk rock and mineral $\delta^{18}\text{O}$ values

The $\delta^{18}\text{O}$ values ($n = 63$) measured in whole rock and mineral separates from peralkaline granites, quartzolites and host rocks range between -8 and $+6\text{‰}$. The spatial distribution of results across the igneous contacts is shown in Fig. 3 and the $\delta^{18}\text{O}$ values are summarized in Fig. 4 according to rock type. The data are reported in Supplementary Table 1. Notably, all 63 samples from different parts of the Keivy magmatic system across 120 km display low $\delta^{18}\text{O}$ values. Quartz and whole rock values of the peralkaline granites are always within 0.2–0.5‰ of each other, and thus, quartz can be taken as a good indicator of the whole rock values.

Quartz extracted from granites has $\delta^{18}\text{O}$ ranging between -0.5 and $+5.5\text{‰}$ (Fig. 4), below the range of typical mantle and crustal rocks between $+6$ and $+10\text{‰}$ (Taylor, 1977). The extreme low $\delta^{18}\text{O}$ values are measured in contact-proximal granites of the Lavrentievskii locality with whole rock values reaching -6‰ . The lowest $\delta^{18}\text{O}$ values are measured in the host gneisses at the West Keivy and Lavrentievskii localities (samples PB172 and LV50V). In these samples, amphibole has a value of -7.8‰ . The bulk measurement in PB172 yields $\delta^{18}\text{O} = -6.5\text{‰}$, while garnet from LV50V has $\delta^{18}\text{O} = -7.3\text{‰}$. Further, quartz-amphibole paired measurements from granites consistently display $+4 - 6\text{‰}$ fractionation. Zircon separates from the granites vary in the range between -0.8 and $+2.1\text{‰}$. Zircon separates from sample of peralkaline granite PM8, which show particularly well-preserved igneous zoning in CL, were run twice and the analyses returned statistically indistinguishable values in the range $+1.7-1.8\text{‰}$. These values are comparable to the $+2.1\text{‰}$ value of zircon in sample PM1 from the same locality and to the $+1.8\text{‰}$ value of zircon from sample KV52 from the West Keivy locality. Zircons from the late-stage quartzolites display a large range of $\delta^{18}\text{O}$ between -4 and $+3\text{‰}$. These zircons are very dark optically and in CL images. These features are suggestive

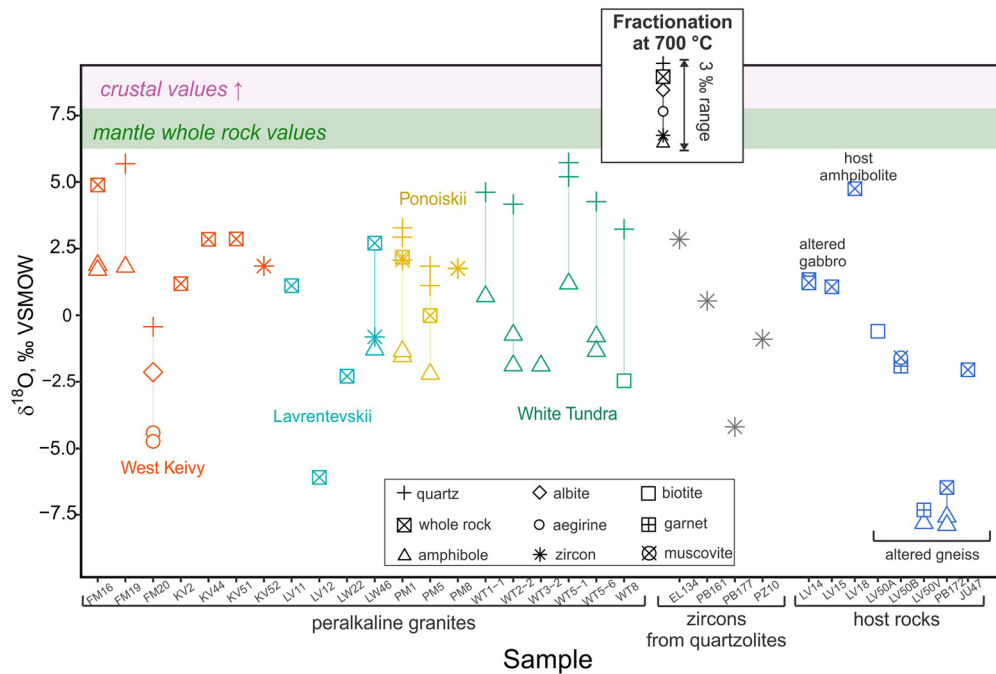


Fig. 4. Oxygen isotope values of mineral separates and whole rock samples measured in Keivy peralkaline granites, host rocks and associated quartzolites. All values measured are below the range of mantle and crustal values typical for silicic rocks (Taylor, 1977; Troch et al., 2020). The calculated equilibrium fractionation between minerals at 700 °C is reported on the same scale in the insert at the top (fractionation factors from Zheng, 1993).

of high U content and potentially high degree of radiation damage and metamictisation, which could lead to post-crystallization O-isotope exchange, and thus it is difficult to assess if zircons from quartzolites actually retain their original $\delta^{18}\text{O}$ values.

4.2. SIMS zircon $\delta^{18}\text{O}$ values

The seven zircon crystals from sample PM8 yield the range of $\delta^{18}\text{O}$ between +1.6 to +2.4‰ (n = 20) with an average of $+2.0 \pm 0.5\text{‰}$ (mean \pm 2SD). The intra-crystal variability ranges between <0.1 to 0.4‰. The data are plotted on selected CL-images and are plotted against the $^{16}\text{OH}/^{16}\text{O}$ values in Fig. 5. The raw data are provided in the Supplementary Table 2. The $^{16}\text{OH}/^{16}\text{O}$ signals range between 0.008 to less than 0.0001. The low $^{16}\text{OH}/^{16}\text{O}$ of several zircons with $\delta^{18}\text{O}$ of +2.3‰ approach that of the 91500 standard grains (see Fig. 5). We take the reproducibility of the values, the agreement between the SIMS and laser fluorination data (within 0.5‰) as well as the low water content of the zircon domains as the reflectors of primary $\delta^{18}\text{O}$ values in sample PM8.

4.3. SIMS zircon U-Pb ages

The U-Pb ages were determined by in situ SIMS measurements of zircons two samples of peralkaline granites, PM8 and WT1-3 corresponding to Ponoiskii and White Tundra localities, respectively, and three late-stage quartzolites from Rovozero (PB161, PB177, PZ10) and one quartz-epidote rock from Elozero (EL134). Zircon crystals are generally euhedral, commonly showing dark and irregular CL emission, and are rich in mineral inclusions (Supplementary Fig. 1). Zircon domains with minimal amount of inclusions and best-preserved regular zoning were targeted for analysis.

In the peralkaline granites, zircon crystals have U contents between 100 and 2400 ppm, and Th/U ratio of 0.03–0.7 (Supplementary Table 3). Many zircon crystals from peralkaline granites returned concordant dates (Fig. 6) for domains with moderate CL emission and visible traces of igneous zoning (Fig. 5A; Supplementary Fig. 1). The average $^{207}\text{Pb}/^{206}\text{Pb}$ age of concordant zircon analyses from sample PM8 (Ponoiskii locality) is 2670 ± 4 Ma

(Concordia age = 2672 ± 7 Ma, Fig. 6). Notably a CL-dark rim of one crystal returned a concordant $^{207}\text{Pb}/^{206}\text{Pb}$ age of 1831 ± 6 Ma (Fig. 5A). Fourteen analyses of zircon in peralkaline granite sample WT1-3 from the White Tundra locality define an upper intercept age of 2672 ± 11 Ma, anchored by a cluster of ten concordant analyses with an average $^{207}\text{Pb}/^{206}\text{Pb}$ age of 2676 ± 3 Ma (MSWD = 0.81). A comparable Neoproterozoic age was measured in zircons from EL134, a quartz-epidote rock from the locality of Elozero (average $^{207}\text{Pb}/^{206}\text{Pb}$ age of 2668 ± 2 Ma).

The zircons from quartzolites with dark CL and faint irregular zoning are visibly more damaged by radioactive decay (Supplementary Fig. 1). Their U concentration ranges between 1200 and 5600 ppm. We attribute the fact that a number of analyses plot above Concordia to this extreme U content compared to that of the standard zircon 91500 and FC1. Consequently, we rely on the $^{207}\text{Pb}/^{206}\text{Pb}$ ages and Discordia intercepts when discussing the quartzolite zircon. Samples from the Rovozero area consistently yield zircon ages in the range between 1770–1800 Ma, but with a scatter of dates above analytical uncertainty. The Discordia intercepts for the Rovozero quartzolites (sample PB161, PB177, PZ10; Fig. 6) are 1766 ± 12 Ma, 1789 ± 10 Ma, and 1792 ± 8 Ma (average $^{207}\text{Pb}/^{206}\text{Pb}$ ages of the oldest group of dates are 1784 ± 8 Ma, 1792 ± 6 Ma, and 1795 ± 2 Ma, respectively). In sample PB161, two inherited zircon cores are dated at 2650–2660 Ma, close to the age of zircon in the peralkaline granites.

In summary, zircon ages pertain to two main geological events. Zircons with magmatic features from two peralkaline granites yield Neoproterozoic ages around 2.67 Ga, which are interpreted to date the crystallization of the granites. These ages agree with the previous determinations that used multi-grain isotope-dilution thermal ionization mass spectrometry (ID-TIMS) to date the White Tundra and West Keivy localities at 2654 ± 5 Ma and 2674 ± 6 Ma, respectively (Zozulya et al., 2005). A previous study reported a zircon upper intercept age of 2666 ± 10 Ma using in situ ion microprobe SHRIMP (Vetrin and Rodionov, 2009) for a granite of the Ponoiskii locality. The Elozero quartz-epidote rock also yields zircon ages similar to that of the granitic emplacement, attesting to likely late magmatic hydrothermal fluids. Quartzolites from Rovozero mainly

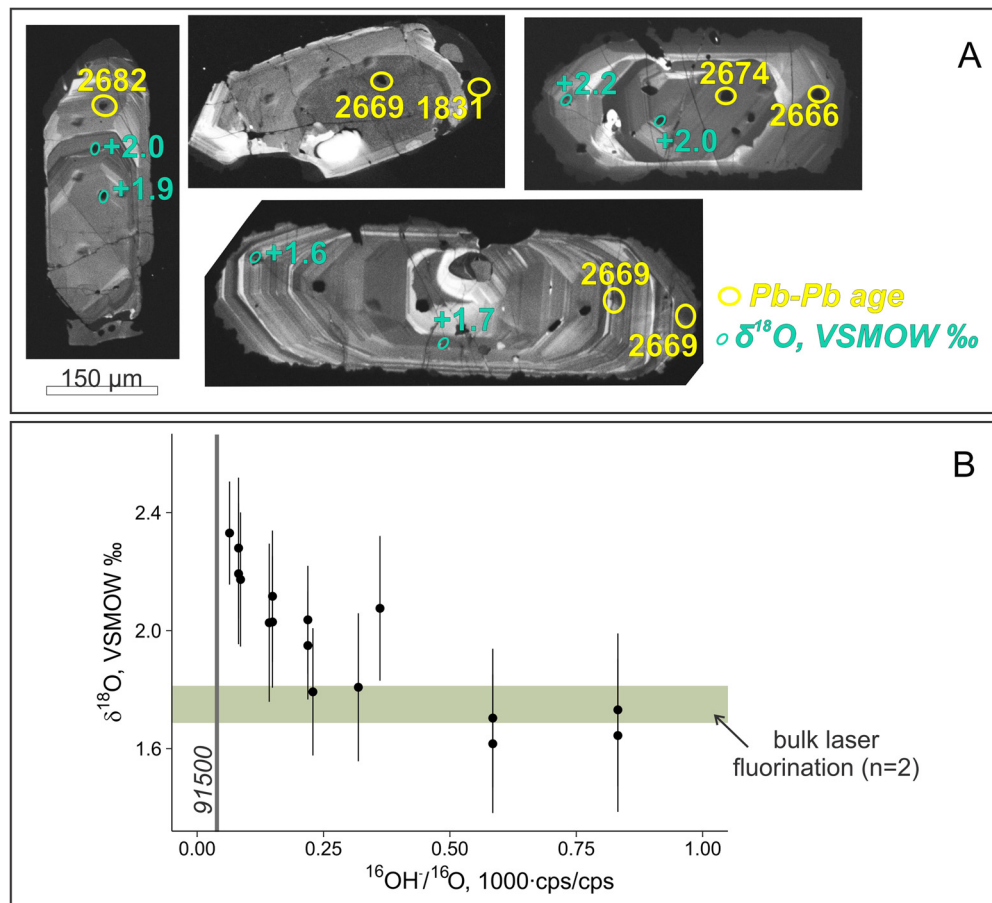


Fig. 5. A – CL-images of representative zircon crystals from the sample PM8 displaying igneous zoning and typical morphology with marked the location of age ($^{207}\text{Pb}/^{206}\text{Pb}$ ages in Ma) and $\delta^{18}\text{O}$ (in ‰ VSMOW) measurements by SIMS. Note the Neoproterozoic age (2669 Ma) of the cores and the Paleoproterozoic age (1831 Ma) of the dark rim in one crystal. The outline of some crystals appears irregular due to the overlay of indium. **B** – The plot of $^{16}\text{OH}/^{16}\text{O}$ versus $\delta^{18}\text{O}$ measured by SIMS in sample PM8. The vertical error bars are 2 σ . The lowest $^{16}\text{OH}/^{16}\text{O}$ signal approaches the signal measured in the standard grains of zircon 91500. The corresponding $\delta^{18}\text{O}$ value is 2.3‰ representing the least altered domains of the PM8 zircons. The laser fluorination measurements (n = 2) of the same sample yield the value of 1.75‰ as shown with a shaded horizontal bar.

contain Paleoproterozoic zircons, with rare Neoproterozoic inheritance. While quartzolites may have initially formed due to granitic emplacement at 2.67 Ga at the contact between granite and country gneisses, the Paleoproterozoic ages between 1.77 and 1.79 Ga are taken to constrain the timing of the last episode of hydrothermal circulation temporally close to the age of regional metamorphism. The schematic diagram showing the envisioned timing of events is shown in Fig. 7.

5. Discussion

5.1. Origin of low- $\delta^{18}\text{O}$ signature in the Keivy granites

All of the $\delta^{18}\text{O}$ values measured in 2.67 Ga Keivy peralkaline granites are low, mostly between 0 and +5‰ in whole rock values and reaching the extreme -6‰ in near-contact aureoles at the Lavrentievskii and West Keivy localities (Fig. 3). The host gneisses values span a similar range, between $\delta^{18}\text{O}$ of ca. -7‰ in the altered gneiss and a near-normal mantle value $\delta^{18}\text{O}$ of +5‰ measured in an amphibolite near the intrusive contact (Fig. 3). The occurrence of low $\delta^{18}\text{O}$ values both in granites and host rocks suggests the syngenetic origin of the O-isotope signature. Given that normal felsic crustal rocks are high in $\delta^{18}\text{O}$ (above ca. +6‰; Taylor, 1977), the low O-isotope signature of Keivy rocks most likely resulted from high-temperature (>300 °C) exchange with low- $\delta^{18}\text{O}$ fluids such as meteoric water.

The widespread low- $\delta^{18}\text{O}$ signature of measured granites indicates they either experienced hydrothermal alteration or formed via assimilation of low- $\delta^{18}\text{O}$ altered rocks. We point out that the low $\delta^{18}\text{O}$ values are measured in all granitic bulk rocks, mineral separates and zircons; thus, this oxygen isotope signature likely comes from igneous assimilation of the pre-existing low- $\delta^{18}\text{O}$ rocks, rather than direct hydrothermal exchanged with low- $\delta^{18}\text{O}$ meteoric waters. This inference is based on measuring low $\delta^{18}\text{O}$ values in unaltered granites from central parts of plutons, where all high-temperature refractory minerals (e.g. quartz, amphibole, zircon) yield low $\delta^{18}\text{O}$ values (Fig. 4). This argument is strengthened by the low $\delta^{18}\text{O}$ of igneous zircons, since the mineral generally retains its primary $\delta^{18}\text{O}$ value over a wide range of geologic conditions including metamorphism and hydrothermal alteration. The well-preserved zircons from the sample of peralkaline granite sample PM8 returned $\delta^{18}\text{O}$ values within +1.7–1.8‰ by bulk laser fluorination, overlapping with the range between +1.6 to +2.4‰ determined by SIMS (Fig. 5). Together with the U-Pb ages of these zircons, their $\delta^{18}\text{O}$ values reflect original magmatic crystallization from a low- $\delta^{18}\text{O}$ magma at 2670 Ma. The pre-existing low- $\delta^{18}\text{O}$ lithologies could have been the altered gneisses, which have the lowest $\delta^{18}\text{O}$ values, down to -7‰ in our collection, and could have been assimilated by normal- $\delta^{18}\text{O}$ magmas (e.g. +7‰; Taylor, 1977). While magmatic assimilation is the most likely mechanism explaining the low $\delta^{18}\text{O}$ values of the unaltered granites, we cannot exclude that some parts of the Keivy granite may have also experienced hydrothermal alteration after emplacement. The second

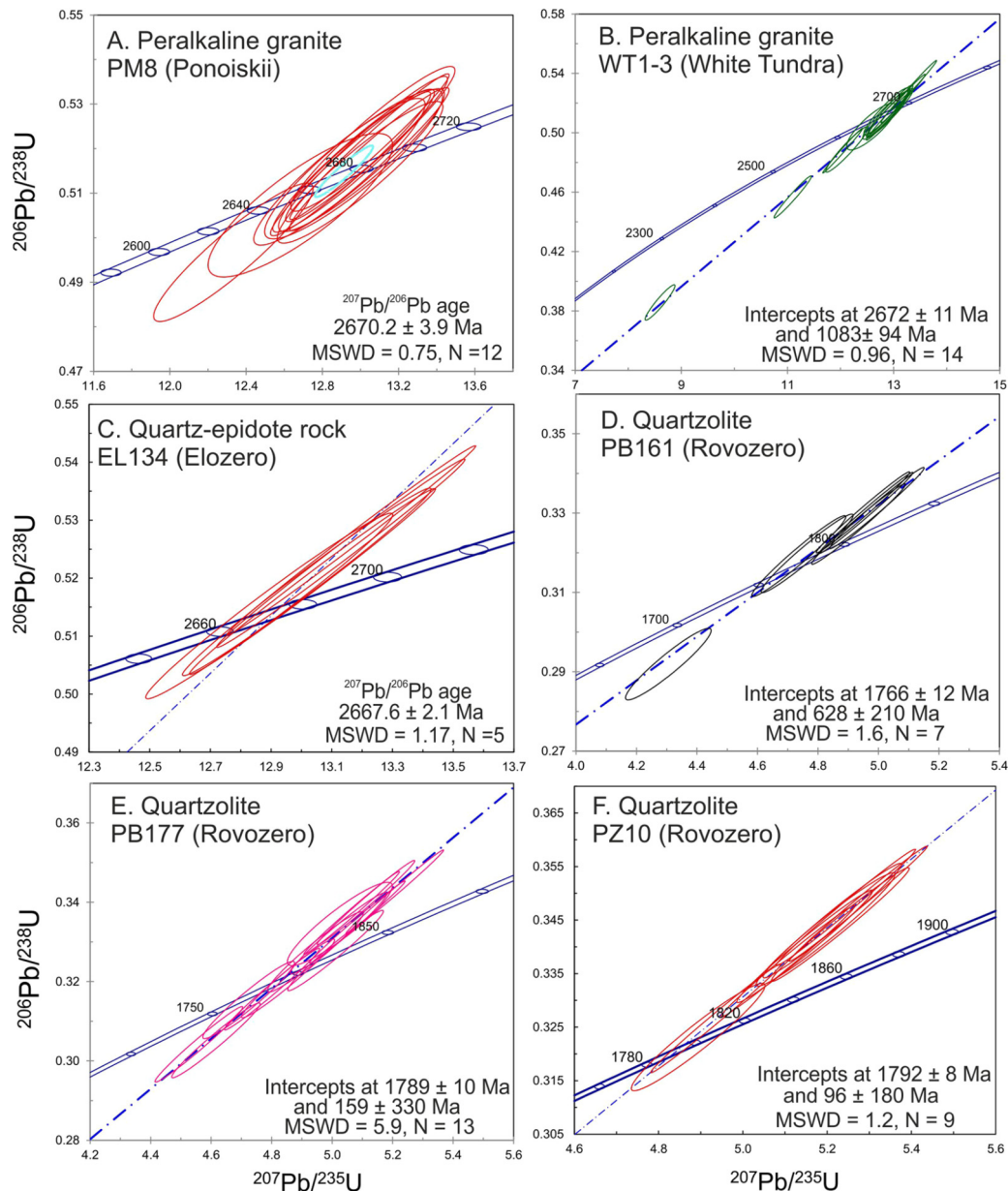


Fig. 6. U-Pb concordia diagrams for SIMS zircon analyses. Error ellipses represent 2-sigma uncertainty. **A** – U-Pb concordia diagram for sample PM8. The cluster of concordant dates defines a Concordia U-Pb age of 2670 ± 4 Ma. **B** – Cluster of concordant zircons along with several zircons that experienced Pb loss from sample WT1-3. Together they define the upper intercept at 2672 ± 11 Ma. **C** – Zircons extracted from the quartz-epidote rock of Elozero locality display a cluster of concordant U-Pb compositions corresponding to ca. 2.67 Ga. **D** through **F** – U-Pb concordia diagrams for zircons extracted from quartzolite localities. The clusters of concordant dates and the upper intercepts define the ages ranging within 1.77–1.79 Ga.

stage of alteration could be recorded for example in the sample LV12 with $\delta^{18}\text{O}$ of -6.1% , which was collected from the contact zone of the Lavrentievskii pluton (see Fig. 3 and 4).

Further, the fact that we find low $\delta^{18}\text{O}$ values in the host rocks in localities ~ 100 km away from each other allows to suggest that the Keivy peralkaline system represent a large and thus likely long-lived (several Myr yet within the analytical uncertainty) shallow (< 5 km depth) magmatic-hydrothermal system. The host rocks $\delta^{18}\text{O}$ values span a larger range of values compared to the peralkaline granites, reaching the extreme low values of -7.8% measured in amphiboles of the altered gneisses. It is likely that the host gneisses were low in $\delta^{18}\text{O}$ sometime before the intrusion of the Keivy granites. The contemporaneity of magmatism (both mafic and granitic) at 2.67 Ga (Zozulya et al., 2005) suggests that the hydrothermal circulation and magmatic emplacement occurred closely in time, likely within several Ma. Further, the lowest $\delta^{18}\text{O}$

values are measured in the host gneisses closest to the contact with peralkaline granites and they bear a clear evidence of alteration in form of blue hastingsite porphyroblasts (Figs. 2 and 3). These features of alteration are spatially intrinsic to the areas near the contacts with peralkaline granites, representing the aureoles of hydrothermal influence within the host rocks. Thus, we opt for the simplest scenario and suggest that the alteration of the host gneisses was near-contemporaneous with emplacement of the granites and magmatic assimilation of the low- $\delta^{18}\text{O}$ lithologies at depth of several km. At such depths, the crust is brittle, allowing circulation of meteoric water around cooling plutons (Ingebritsen and Manning, 1999).

The O-isotope fractionations between the co-existing minerals indicate that equilibrium (if achieved) was established below the granitic solidus at around 700°C (see Fig. 4). The regional amphibolite-facies metamorphism at ca. 1.8 Ga is the most likely

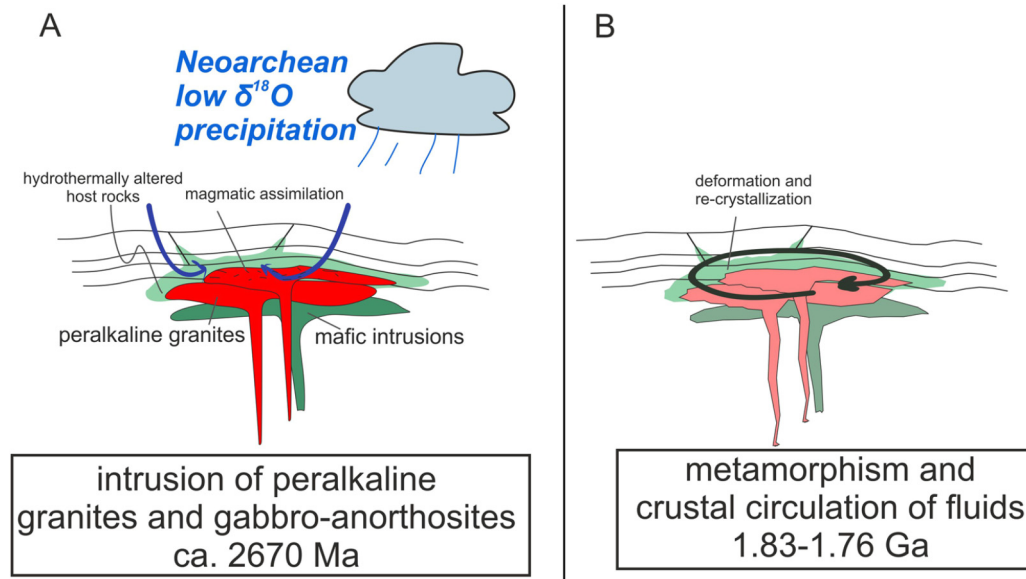


Fig. 7. A schematic cartoon representing the envisaged chronological evolution of the Keivy magmatic-hydrothermal system as inferred from this study. **A** – Neoproterozoic emplacement of the mafic intrusions (dark green) and peralkaline granites (red) in the volcanic and sedimentary units (shown as wavy white layers) of Keivy terrane, Kola craton. Both mafic and peralkaline granitic magmatism is dated to 2.67 Ga. The shallow (several km depth) emplacement of magmas promoted hydrothermal circulation of the local low- $\delta^{18}\text{O}$ precipitation that induced hydrothermal alteration of the host rocks to low $\delta^{18}\text{O}$. Magmatic assimilation likely occurred within several Ma introducing low $\delta^{18}\text{O}$ values in granitic magmas. **B** – The regional metamorphism at ca. 1.8 Ga induced recrystallization of all units of the Keivy terrane including the low $\delta^{18}\text{O}$ altered host rocks and granites. Metamorphism is likely responsible for the observed mineral $\delta^{18}\text{O}$ fractionations (see Fig. 4). Quartzolites dated here to roughly 1.8–1.7 Ga depict late-stage fluid cycling near-contemporaneously with regional metamorphism.

reason for the observed fractionation between individual minerals. Yet, the influence of metamorphism is unlikely to be responsible for the regionally observed low $\delta^{18}\text{O}$ values. In general, metamorphism in a closed system does not alter the bulk rock $\delta^{18}\text{O}$ signature, so that metamorphic rocks maintain their protolith bulk oxygen composition. Moreover, it is difficult to alter $\delta^{18}\text{O}$ values regionally during metamorphic recrystallization because O is a major element ($\sim 45\text{--}50\text{ wt.}\%$) in silicate rocks. Thus, while individual mineral phase reflects re-distribution of $\delta^{18}\text{O}$ values under amphibolite facies ($\sim 500\text{ }^\circ\text{C}$) at 1.8 Ga either due to O diffusion or due to solid-state recrystallization, the low $\delta^{18}\text{O}$ whole rock values still depict the pre-metamorphic origin of the meteoric water-rock exchange.

5.2. Comparison to recent magmatic-hydrothermal systems

Tentatively, the geological situation represents a large sub-volcanic complex, similar to the more recent low- $\delta^{18}\text{O}$ systems of the Cenozoic, where O isotope depletion is measured in the host rocks and within the intrusions themselves. Some of the well-studied examples include the Tertiary intrusion of Skaergaard (Taylor and Forester, 1979), granites of the Cascades (Taylor, 1971), and the Isle of Skye complex (Monani and Valley, 2001). In these shallow magmatic-hydrothermal systems, low- $\delta^{18}\text{O}$ lithologies were generated in the host rocks as well as within the intrusions. Some of the minerals within the intrusions represent original low- $\delta^{18}\text{O}$ unaltered igneous phases (e.g. quartz phenocrysts and zircons), presenting evidence for their crystallization from low- $\delta^{18}\text{O}$ magmas (e.g. granites from the Isle of Skye; Monani and Valley, 2001). At the same time, secondary minerals, healed cracks, feldspars, sub-solidus overgrowths that develop within intrusions (e.g. Valley and Graham, 1996) and within the altered host rocks also have low $\delta^{18}\text{O}$ values due to exchange with the low- $\delta^{18}\text{O}$ meteoric waters via hydrothermal cycling. If enough heat is provided, the generated materials can be remelted and assimilated in repeated episodes of magmatism and/or during late-stage in situ re-melting (Bindeman et al., 2008; Wotzlaw et al., 2012; Troch et al., 2020). Syn-

magmatic hydrothermal alteration to low $\delta^{18}\text{O}$ values and igneous assimilation is documented in multiple plutonic and volcanic environments spanning in age from about 1080 Ma to the Holocene, with the magmatic $\delta^{18}\text{O}$ values ranging from -1 to $+6\text{‰}$ (see review in Troch et al., 2020). In summary, we document one of the earliest examples of such interaction between shallow stored magma and surface waters, where magmas were likely emplaced as low $\delta^{18}\text{O}$ due to recycling of low- $\delta^{18}\text{O}$ hydrothermally altered rocks. This marks the 2.67 Ga Keivy magmatic-hydrothermal complex as one of the earliest low- $\delta^{18}\text{O}$ systems documenting an active hydrological cycle in the Archean over exposed continental crust.

5.3. Timing of igneous emplacement, alteration and emplacement of quartzolites

The new U-Pb zircon ages allow us to depict the order of events pertinent to the emplacement of low- $\delta^{18}\text{O}$ granites and hydrothermal alteration of the host rocks (see Fig. 6). We show that the peralkaline granite intrusions are constrained to $2672 \pm 7\text{ Ma}$ at the White Tundra and Ponoiskii localities, in agreement with previous studies that determined the ages of peralkaline granites as well as the near-contemporaneous mafic intrusions (Bayanova, 2004; Zozulya et al., 2005; Vetrin and Rodionov, 2009). The chronology is particularly important for sample PM8, as the zircons produce concordant U-Pb dates, display igneous zoning in CL-images, and consistently reproduce low $\delta^{18}\text{O}$ values. Further, we provide the first U-Pb ages for the quartzolites hosted in the Keivy magmatic system. A quartz-epidote rock from the Elozero locality contains zircon with $\sim 2.67\text{ Ga}$ concordant ages overlapping with the magmatic stage of the Keivy terrane. This age depicts the original $\delta^{18}\text{O}$ water-rock interaction that was likely induced by the peralkaline granitic magmatism (Fig. 6). On the other hand, the Rovozero quartzolite of the West Keivy locality contains zircons that yield ages of 1.77–1.79 Ga, significantly post-dating the emplacement of granites. These ages represent either the emplacement of quartzolites or resetting of the zircon ages during a later re-mobilization event.

5.4. Implications for continental exposure and hydrological cycle at ca. 2.67 Ga

Our suite of samples indicates that the meteoric water precipitated over the continental crust and was entrained in hydrothermal exchange reactions on the Kola craton at 2.67 Ga. This inference relies on the negative $\delta^{18}\text{O}$ values measured in rocks and minerals that underwent high-temperature exchange with surface fluids because meteoric water is the main reservoir of negative $\delta^{18}\text{O}$ values (Taylor, 1977). Since meteoric water is derived from evaporation of seawater, it is plausible that the low $\delta^{18}\text{O}$ value of Neoproterozoic seawater was the determining factor for the observed negative values in the Keivy complex. Such argument is prompted by the long-lasting controversy surrounding the $\delta^{18}\text{O}$ evolution of seawater, since Precambrian marine cherts and carbonates are 10–15‰ lower in $\delta^{18}\text{O}$ compared to the more recent counterparts (Knauth, 2005; Jaffrés et al., 2007). Based on the growing number of studies that utilize multi-isotope systems, e.g. triple O isotopes that constrain both temperature and fluid sources (Sengupta et al., 2020; Wostbrock and Sharp, 2021; Zakharov et al., 2021), the influence of diagenesis remains among the strongest factors that explain the low $\delta^{18}\text{O}$ values of Precambrian marine records. Moreover, the studies of early Precambrian submarine altered mafic rocks that focused on reconstructing the seawater isotope values at ~2.7 Ga (Peters et al., 2020) and at 2.41 Ga (Zakharov and Bindeman, 2019) yielded seawater $\delta^{18}\text{O}$ values of ca. -1 and -2 ‰, respectively. Thus, it is reasonable to assume that the $\delta^{18}\text{O}$ value seawater was not significantly different at 2.7 Ga (within ± 2 ‰), and that the low $\delta^{18}\text{O}$ values recorded in the Keivy system are due to subaerial exposure of the Kola craton allowing for interaction with 2.67 Ga meteoric waters.

Since the lowest $\delta^{18}\text{O}$ values of -8 to -7 ‰ were measured in the samples of altered host rocks (samples PB172 and LV50V), we infer that the equilibrium fluid had ca. -9 ‰, as mineral-water fractionation at the hydrothermal temperature range (300–400 °C) is at least $+2$ ‰. This fractionation presents a conservative estimate assuming that pre-metamorphic assemblages were, for example, a mixture of albite and actinolite with fractionation factors of $+3.3$ and -0.7 ‰ at 350 °C, respectively (see Zheng, 1993); the exact mineral-water fractionation is dependent on the exact mineral composition of the hydrothermally altered rock at 2.67 Ga (prior to metamorphism), which is now difficult to establish. The value of -9 ‰ is a maximum estimate for the $\delta^{18}\text{O}$ value of contemporaneous meteoric water, as $\delta^{18}\text{O}$ of hydrothermal fluids are typically modified towards heavier values due to reaction with rocks that have comparatively high $\delta^{18}\text{O}$ values. In modern continental hydrothermal systems, the $\delta^{18}\text{O}$ values are shifted according to water/rock ratios of around 0.5–4 (Cole, 1994). If we assume an average water/rock ratio of 2, then the initial meteoric water would have had $\delta^{18}\text{O} = -11$ ‰.

Today a $\delta^{18}\text{O}$ value of -11 ‰ in meteoric water corresponds to the inland regions of the world, mostly in the Northern Hemisphere, north of latitude 40° (Rozanski et al., 1993; Bowen et al., 2005). For example, such $\delta^{18}\text{O}$ of precipitation is found in the Mid-Western United States, but also in the elevated areas of the world, e.g. foothills of Tibetan Plateau in China and in the waters feeding Lake Geneva in Switzerland. Using the strong linear relationship between mean annual temperature and $\delta^{18}\text{O}$ of precipitation (Dansgaard, 1964) as a broad approximation, such values are observed in the regions with mean annual temperatures of around 4 °C or lower. Thus, the reconstructed meteoric water with $\delta^{18}\text{O}$ of at least -11 ‰ could represent to a diverse set of geographic locations. The paleogeographic location of the Kola craton is constrained to high-latitudes of 80–70° via paleomagnetic studies of a suite of rocks that formed at 2.68–2.63 Ga (Salminen et al., 2021). Together with these paleogeographic data, our newly derived proxy

documents a $\delta^{18}\text{O}$ value of meteoric water in the Neoproterozoic polar regions. If the modern relationship between mean annual temperature and $\delta^{18}\text{O}$ of meteoric water (Dansgaard, 1964) remains valid for the Neoproterozoic climate systems, then the region was characterized by the mean annual temperatures of 4 °C or lower. The reconstructed signature indicates that parts of the Neoproterozoic world hosted cool climate conditions. Further, this is supported by the Neoproterozoic glaciation episode as documented by the 2.7 Ga continentally deposited diamictites (Ojakangas et al., 2014).

In addition, the paleopoles derived from the Neoproterozoic formations of the Superior craton (Canadian Shield) indicate its connection or proximity to the Kola-Karelia craton (e.g. Salminen et al., 2021), forming the Superia supercraton along with Hearne, Kaapvaal, and Wyoming cratons (Liu et al., 2021 and references therein). In this view, our newly constructed proxy for ancient precipitation has an important paleogeographic implication. It could be tested whether or not other proximal cratons contain a record of 2.67 Ga meteoric water, potentially documenting a spatial extent of the continental exposure. Since the meteoric water $\delta^{18}\text{O}$ value has a strong latitude control, contemporaneous low- $\delta^{18}\text{O}$ magmatic-hydrothermal systems can be used as a tool to test for cratonic connections. Insofar, however, other hints to Archean shallow magmatic-hydrothermal systems are rare and only documented by low $\delta^{18}\text{O}$ of zircons from metamorphosed or clastic formations (Hammerli et al., 2018; Spencer et al., 2019; Wang et al., 2021) qualitatively attesting to the sub-aerial exposure of continental crust. In this light, the 2.67 Ga low- $\delta^{18}\text{O}$ Keivy granites and their host rocks of the Kola craton present one of the earliest 'intact' continental hydrothermal-magmatic systems that offers a quantitative insight into the early hydrologic cycle.

6. Conclusions

We document a Neoproterozoic continental magmatic-hydrothermal system from the Keivy granite complex, Kola craton. Local precipitation with $\delta^{18}\text{O} \leq -11$ ‰ is recorded through hydrothermal alteration likely caused by emplacement of peralkaline granitic magmas in an anorogenic environment at 2.67 Ga. The detailed $\delta^{18}\text{O}$ mapping, O-isotope mineral-pair thermometry and secondary ion microprobe U-Pb dating of zircons build the case for syn-emplacement alteration in presence of local meteoric water and magmatic assimilation of hydrothermally altered rocks. In summary, we found:

1. The scale of O isotope depletion spans at least 120 km in length across different lithological units that include the peralkaline granites of the Keivy complex, associated quartzolites and the hosting gneisses. The lowest $\delta^{18}\text{O}$ values of ca. -7 ‰ are measured in the altered gneisses near the intrusive contacts. Peralkaline granites themselves returned $\delta^{18}\text{O}$ values ranging between -6 and $+5$ ‰.
2. U-Pb dating of igneous zircons reveals that the studied plutonic rocks were emplaced at 2.67 Ga. The average Concordia ages of well-preserved magmatic zircons from the two localities of White Tundra and Ponoiskii are 2672 ± 7 Ma. One quartz-epidote rock from the locality of Elozero returned an age similar to that of the igneous emplacement at 2.67 Ga, depicting the syn-emplacement water-rock interaction. Zircons from the quartzolites trace the late-stage mobilization/recrystallization and yield U-Pb ages of 1.77–1.79 Ga, temporally close to the age of regional metamorphism.
3. We interpret that the low $\delta^{18}\text{O}$ signature of the peralkaline granites and the host rocks formed in the shallow crust at 2672 Ma. The spatially extensive O-isotope depletion resulted from interaction between the hot crust and local precipitation. Some remelting and assimilation of the low- $\delta^{18}\text{O}$ al-

tered lithologies occurred as documented by low $\delta^{18}\text{O}$ values measured in preserved igneous zircons. Further, samples of the hosting gneisses spatially spanning over 100 km exhibit low $\delta^{18}\text{O}$ with the lowest $\delta^{18}\text{O}$ values found in the contact-proximal areas.

- We estimate the equilibrium fluids had $\delta^{18}\text{O}$ of maximum -9‰ under hydrothermal conditions and the contemporaneous precipitation had $\delta^{18}\text{O} = -11\text{‰}$ or lower. In the modern world, precipitation with such low $\delta^{18}\text{O}$ values occur in regions with polar climate with mean annual temperature of around 4°C . Combined with the high-latitude position of the Kola craton ($80\text{--}70^\circ$), the 2.67 Ga Keivy granites provide one of the earliest quantitative records of precipitation over exposed continental crust.

CRediT authorship contribution statement

David Zakharov designed the study, collected oxygen isotope and U-Pb data, and wrote the original manuscript.

Dmitry Zozulya designed the study and collected samples for the study. Daniela Rubatto designed the study and collected U-Pb data.

All authors contributed to editing the manuscript and figures.

Declaration of competing interest

The authors declare that they have no known competing financial interests or personal relationships that could have appeared to influence the work reported in this paper.

Acknowledgements

Authors acknowledge funding from the Faculty of Geosciences and Environment (FGSE), University of Lausanne to DZ, Russian Government Grant 0226-2019-0053 to DRZ, and Swiss National Science Foundation (SNSF) grant 191959 to DR. We thank Torsten Vennemann for granting access to the Stable Isotope Laboratory at the University of Lausanne and Benita Putlitz for the laboratory assistance. Johanna Marin-Carbonne is thanked for supporting this project. We also thank Ilya Bindeman for facilitating the early preliminary $\delta^{18}\text{O}$ measurements at the fluorination line in University of Oregon. The Hyperion source of the SwissSIMS instrument used for U-Pb geochronology was partially supported by the FGSE and SNSF. We are thankful for the thoughtful reviews provided by Daniel Herwartz and Juliana Troch. We also thank the handling editor Boswell Wing.

Appendix A. Supplementary material

Supplementary material related to this article can be found online at <https://doi.org/10.1016/j.epsl.2021.117322>.

References

Bagiński, B., Zozulya, D., Macdonald, R., Kartashov, P.M., Dzierżanowski, P., 2016. Low-temperature hydrothermal alteration of a rare-metal rich quartz-epidote metamatite from the El'zero deposit, Kola Peninsula, Russia. *Eur. J. Mineral.* 28, 789–810.

Balagansky, V.V., Myskova, T.A., Lvov, P.A., Larionov, A.N., Gorbunov, I.A., 2021. Neoproterozoic A-type acid metavolcanics in the Keivy Terrane, northeastern Fennoscandian Shield: geochemistry, age, and origin. *Lithos* 380, 105899.

Batieva, I.D., 1976. Petrology of Alkaline Granitoids of the Kola Peninsula. Nauka, St. Petersburg.

Bayanova, T.B., 2004. Age of Reference Geological Complexes of the Kola Region and Duration of Magmatic Processes. Nauka, St. Petersburg.

Bindeman, I.N., Fu, B., Kita, N.T., Valley, J.W., 2008. Origin and evolution of silicic magmatism at Yellowstone based on ion microprobe analysis of isotopically zoned zircons. *J. Petrol.* 49, 163–193.

Bindeman, I.N., Zakharov, D.O., Palandri, J., Greber, N.D., Dauphas, N., Retallack, G.J., Hofmann, A., Lackey, J.S., Bekker, A., 2018. Rapid emergence of subaerial landmasses and onset of a modern hydrologic cycle 2.5 billion years ago. *Nature* 557, 545–548.

Bowen, G.J., Wassenaar, L.I., Hobson, K.A., 2005. Global application of stable hydrogen and oxygen isotopes to wildlife forensics. *Oecologia* 143, 337–348.

Catling, D.C., Zahnle, K.J., 2020. The Archean atmosphere. *Sci. Adv.* 6, eaax1420.

Cole, D.R., 1994. Evidence for oxygen isotope disequilibrium in selected geothermal and hydrothermal ore deposit systems. *Chem. Geol.* 111, 283–296.

Craig, H., 1961. Isotopic variations in meteoric waters. *Science, New Ser.* 133, 1702–1703.

Dansgaard, W., 1964. Stable isotopes in precipitation. *Tellus* 16, 436–468.

Dhuime, B., Hawkesworth, C.J., Cawood, P.A., Storey, C.D., 2012. A change in the geodynamics of continental growth 3 billion years ago. *Science* 335, 1334–1336.

Flament, N., Coltice, N., Rey, P.F., 2008. A case for late-Archaean continental emergence from thermal evolution models and hypsometry. *Earth Planet. Sci. Lett.* 275, 326–336.

Hammerli, J., Kemp, A.I., Jeon, H., 2018. An Archean Yellowstone? Evidence from extremely low $\delta^{18}\text{O}$ in zircons preserved in granulites of the Yilgarn Craton, Western Australia. *Geology* 46, 411–414.

Ingebritsen, S.E., Manning, C.E., 1999. Geological implications of a permeability-depth curve for the continental crust. *Geology* 27, 1107–1110.

Jaffrés, J.B.D., Shields, G.A., Wallmann, K., 2007. The oxygen isotope evolution of seawater: a critical review of a long-standing controversy and an improved geological water cycle model for the past 3.4 billion years. *Earth-Sci. Rev.* 83, 83–122.

Johnson, B.W., Wing, B.A., 2020. Limited Archean continental emergence reflected in an early Archean 18 O-enriched ocean. *Nat. Geosci.* 13, 243–248.

Jourdan, A.-L., Vennemann, T.W., Mullis, J., Ramseyer, K., 2009. Oxygen isotope sector zoning in natural hydrothermal quartz. *Mineral. Mag.* 73, 615–632.

Knauth, P.L., 2005. Temperature and salinity history of the Precambrian ocean: implications for the course of microbial evolution. *Palaeogeogr. Palaeoclimatol. Palaeoecol.* 219, 53–69.

Liu, Y., Mitchell, R.N., Li, Z.-X., Kirscher, U., Pisarevsky, S.A., Wang, C., 2021. Archean geodynamics: ephemeral supercontinents or long-lived supercratons. *Geology*.

Ludwig, K.R., 2003. User's Manual for Isoplot 3.00, a Geochronological Toolkit for Microsoft Excel. Berkeley Geochronol. Cent. Spec. Publ., vol. 4, pp. 25–32.

Macdonald, R., Bagiński, B., Zozulya, D., 2017. Differing responses of zircon, chevkinite-(Ce), monazite-(Ce) and fergusonite-(Y) to hydrothermal alteration: evidence from the Keivy alkaline province, Kola Peninsula, Russia. *Mineral. Petrol.* 111, 523–545.

Monani, S., Valley, J.W., 2001. Oxygen isotope ratios of zircon: magma genesis of low $\delta^{18}\text{O}$ granites from the British Tertiary Igneous Province, western Scotland. *Earth Planet. Sci. Lett.* 184, 377–392.

Ojakangas, R.W., Srinivasan, R., Hegde, V.S., Chandrakant, S.M., Srikantia, S.V., 2014. The Talya conglomerate: an Archean (2.7 Ga) glaciomarine formation, Western Dharwar Craton, Southern India. *Curr. Sci.*, 387–396.

Paces, J.B., Miller, J.D., 1993. Precise U-Pb ages of Duluth complex and related mafic intrusions, northeastern Minnesota: geochronological insights to physical, petrogenetic, paleomagnetic, and tectonomagmatic processes associated with the 1.1 Ga midcontinent rift system. *J. Geophys. Res., Solid Earth* 98, 13997–14013.

Peters, S.T., Szilas, K., Sengupta, S., Kirkland, C.L., Garbe-Schönberg, D., Pack, A., 2020. >2.7 Ga metamorphic peridotites from southeast Greenland record the oxygen isotope composition of Archean seawater. *Earth Planet. Sci. Lett.* 544, 116331.

Rozanski, K., Araguás-Araguás, L., Gonfiantini, R., 1993. Isotopic patterns in modern global precipitation. In: *Climate Change in Continental Isotopic Records*, vol. 78, pp. 1–36.

Salminen, J., Lehtonen, E., Mertanen, S., Pesonen, L.J., Elming, S.-Å., Luoto, T., 2021. Chapter 5 - the Precambrian drift history and paleogeography of Baltica. In: Pesonen, L.J., Salminen, J., Elming, S.-Å., Evans, D.A.D., Veikkolainen, T. (Eds.), *Ancient Supercontinents and the Paleogeography of Earth*. Elsevier, pp. 155–205.

Sengupta, S., Peters, S.T.M., Reitner, J., Duda, J.-P., Pack, A., 2020. Triple oxygen isotopes of cherts through time. *Chem. Geol.* 554, 119789.

Spencer, C.J., Partin, C.A., Kirkland, C.L., Raub, T.D., Liebmann, J., Stern, R.A., 2019. Paleoproterozoic increase in zircon $\delta^{18}\text{O}$ driven by rapid emergence of continental crust. *Geochim. Cosmochim. Acta* 257, 16–25.

Stacey, J.S., Kramers, J.D., 1975. Approximation of terrestrial lead isotope evolution by a two-stage model. *Earth Planet. Sci. Lett.* 26, 207–221.

Taylor, H.P., 1971. Oxygen isotope evidence for large-scale interaction between meteoric ground waters and Tertiary granodiorite intrusions, Western Cascade Range, Oregon. *J. Geophys. Res.* 76, 7855–7874.

Taylor, H.P., 1977. Water/rock interactions and the origin of H₂O in granitic batholiths: thirtieth William Smith lecture. *J. Geol. Soc.* 133, 509–558.

Taylor, H.P., Forester, R.W., 1979. An oxygen and hydrogen isotope study of the Skaergaard intrusion and its country rocks: a description of a 55 M.Y. old fossil hydrothermal system. *J. Petrol.* 20, 355–419.

Troch, J., Ellis, B.S., Harris, C., Bachmann, O., Bindeman, I.N., 2020. Low- $\delta^{18}\text{O}$ silicic magmas on Earth: a review. *Earth-Sci. Rev.* 208, 103299.

Valley, J.W., Graham, C.M., 1996. Ion microprobe analysis of oxygen isotope ratios in quartz from Skye granite: healed micro-cracks, fluid flow, and hydrothermal exchange. *Contrib. Mineral. Petrol.* 124, 225–234.

- Vetrin, V.R., Rodionov, N.V., 2009. Geology and geochronology of Neoproterozoic anorogenic magmatism of the Keivy structure, Kola Peninsula. *Petrology* 17, 537–557.
- Wang, W., Cawood, P.A., Spencer, C.J., Pandit, M.K., Zhao, J.-H., Xia, X.-P., Zheng, J.-P., Lu, G.-M., 2021. Global-scale emergence of continental crust during the Mesoproterozoic–early Neoproterozoic. *Geology*.
- Watts, K.E., Bindeman, I.N., Schmitt, A.K., 2012. Crystal scale anatomy of a dying supervolcano: an isotope and geochronology study of individual phenocrysts from voluminous rhyolites of the Yellowstone caldera. *Contrib. Mineral. Petrol.* 164, 45–67.
- Wiedenbeck, M., Hanchar, J.M., Peck, W.H., Sylvester, P., Valley, J., Whitehouse, M., Kronz, A., Morishita, Y., Nasdala, L., Fiebig, J., 2004. Further characterisation of the 91500 zircon crystal. *Geostand. Geoanal. Res.* 28, 9–39.
- Winnick, M.J., Chamberlain, C.P., Caves, J.K., Welker, J.M., 2014. Quantifying the isotopic 'continental effect'. *Earth Planet. Sci. Lett.* 406, 123–133.
- Wostbrock, J.A.G., Sharp, Z.D., 2021. Triple Oxygen Isotopes in Silica–Water and Carbonate–Water Systems. *Reviews in Mineralogy and Geochemistry*, vol. 86, pp. 367–400.
- Wotzlaw, J.-F., Bindeman, I.N., Schaltegger, U., Brooks, C.K., Naslund, H.R., 2012. High-resolution insights into episodes of crystallization, hydrothermal alteration and remelting in the Skaergaard intrusive complex. *Earth Planet. Sci. Lett.* 355–356, 199–212.
- Zakharov, D.O., Bindeman, I.N., 2019. Triple oxygen and hydrogen isotopic study of hydrothermally altered rocks from the 2.43–2.41 Ga Vetreny belt, Russia: an insight into the early Paleoproterozoic seawater. *Geochim. Cosmochim. Acta* 248, 185–209.
- Zakharov, D.O., Bindeman, I.N., Tanaka, R., Friðleifsson, G.Ó., Reed, M.H., Hampton, R.L., 2019. Triple oxygen isotope systematics as a tracer of fluids in the crust: a study from modern geothermal systems of Iceland. *Chem. Geol.* 530, 119312.
- Zakharov, D.O., Marin-Carbonne, J., Alleon, J., Bindeman, I.N., 2021. Triple oxygen isotope trend recorded by Precambrian cherts: a perspective from combined bulk and in situ secondary ion probe measurements. *Rev. Mineral. Geochem.* 86, 323–365.
- Zheng, Y.-F., 1993. Calculation of oxygen isotope fractionation in hydroxyl-bearing silicates. *Earth Planet. Sci. Lett.* 120, 247–263.
- Zozulya, D., Macdonald, R., Bagiński, B., 2020. REE fractionation during crystallization and alteration of fergusonite-(Y) from Zr-REE-Nb-rich late-to post-magmatic products of the Keivy alkali granite complex, NW Russia. *Ore Geol. Rev.*, 103693.
- Zozulya, D.R., Bayanova, T.B., Eby, G.N., 2005. Geology and age of the Late Archean Keivy alkaline province, northeastern Baltic Shield. *J. Geol.* 113, 601–608.